

Article

Bionic ankle-assisted rehabilitation training system based on biomechanical evaluation

Jiandong Wang¹, Yuanwei Li^{2,*}, Baoku Sui³¹ Department of Physical Education and Research, The Tourism College of Changchun University, Changchun 130607, Jilin, China² Department of Basic Courses, Wuhan Qingchuan University, Wuhan 430204, Hubei, China³ School of Winter Sports, Capital University of Physical Education and Sports, Beijing 100191, China* **Corresponding author:** Yuanwei Li, liyuanwei1011@163.com

CITATION

Wang J, Li Y, Sui B. Bionic ankle-assisted rehabilitation training system based on biomechanical evaluation. *Molecular & Cellular Biomechanics*. 2024; 21(2): 236. <https://doi.org/10.62617/mcb.v21i2.236>

ARTICLE INFO

Received: 8 July 2024

Accepted: 16 August 2024

Available online: 6 November 2024

COPYRIGHT



Copyright © 2024 by author(s).

Molecular & Cellular Biomechanics

is published by Sin-Chn Scientific Press Pte. Ltd. This work is licensed

under the Creative Commons

Attribution (CC BY) license.

<https://creativecommons.org/licenses/by/4.0/>

Abstract: In modern society, people's life rhythm is getting faster and faster. Ankle injury would significantly reduce the frequency of people's activities, which has a great impact on people's normal work and life. As a new medical method, the bionic ankle rehabilitation training system is used to assist rehabilitation doctors to help patients complete joint flexibility and recovery training. In the research method of ankle biomechanical characteristics, the detection of ankle joint patient's motion is particularly important. The purpose of this paper is to study how to design a bionic ankle assisted rehabilitation training system based on image processing. Therefore, this paper proposes an image-based moving target detection method, which has the advantages of high reliability and simple operation, and can improve the recognition rate of the ankle joint movement. The experimental results of this paper showed that the system can realize the predetermined trajectory movement and run the system stably. In terms of patient following error, it was kept within 0.03cm. The following error of the ankle joint trajectory was up to 0.03cm and the lowest was 0.01cm, which was almost negligible. In terms of accuracy, the accuracy of the system was also very high, and it can respond and determine the patient's actions quickly, thereby helping patients to better perform rehabilitation training.

Keywords: bionic ankle; image processing; object detection; rehabilitation training system

1. Introduction

Ankle injuries are common in sports, often ranking second among lower limb injuries. Activities like running and jumping place significant loads on the ankle, increasing the risk of injury, especially in sports with frequent direction changes. Untreated or inadequately treated ankle sprains can lead to ligament laxity, instability, and recurrent injuries, affecting normal walking. Given the frequency of ankle injuries, understanding their mechanical properties is crucial in rehabilitation medicine. This paper introduces an innovative mobile target detection algorithm based on image processing, applied to a bionic ankle-assisted rehabilitation system to improve detection accuracy and accelerate recovery. The system offers personalized rehabilitation plans at different stages: it starts by assessing the patient's initial condition and injury extent, adjusts training intensity and methods in the mid-stage based on real-time data, and focuses on enhancing flexibility and stability in the final stage. This approach significantly improves rehabilitation outcomes and patient experience due to its high reliability and ease of use.

During the system's application phase, patients with ankle joint injuries participated in rehabilitation training aimed at restoring ankle function. Initially, the

system provided passive training with trajectory errors maintained between 0.01cm and 0.03cm. As rehabilitation progressed, it transitioned to active training, improving target detection accuracy. Patients using the system experienced significantly faster recovery and better outcomes compared to those who did not use it, with marked improvements in ankle joint function. The system demonstrates significant advantages in improving rehabilitation efficiency, reducing patient pain, and shortening recovery time. Through precise image processing and moving target detection, the system accurately tracks ankle joint movement and optimizes rehabilitation outcomes. It offers personalized training plans, transitioning from passive to active training, which effectively enhances the speed and effectiveness of recovery. Real-time adjustments to training intensity and methods reduce the risk of injury from insufficient or excessive training and alleviate patient discomfort. Integrating this system with existing rehabilitation methods can create a comprehensive rehabilitation program, further improving efficiency and reducing recovery time, while providing a more thorough and effective rehabilitation experience.

To comprehensively evaluate the effectiveness of this system in clinical applications, a comparative analysis was conducted, including changes in patients' functional scores and pain levels before and after using the system for rehabilitation training. Tracking the rehabilitation of 30 patients with ankle joint injuries revealed significant improvements in the range of motion after 8 weeks of rehabilitation. Using the American Orthopaedic Foot and Ankle Society (AOFAS) Ankle-Hindfoot Scale, the average score for patients before rehabilitation was 65.2 ± 7.8 , which increased to 88.4 ± 5.6 after rehabilitation, with the difference being statistically significant ($P < 0.01$). Additionally, pain levels were assessed using the Visual Analog Scale (VAS), showing an average pain score of 6.3 ± 1.2 before rehabilitation, which decreased to 1.4 ± 0.7 after rehabilitation, also demonstrating a significant statistical difference ($P < 0.01$). These results indicate that the system effectively improves ankle joint function and reduces patient pain. Referring to previously published clinical studies, such as Wang et al.'s 2018 study [1], which noted that robotic ankle rehabilitation significantly enhances patient recovery, this system shows promise. However, compared to existing technologies, the system's stability and durability over long-term use need further verification. Future efforts will focus on enhancing the system's personalization capabilities and developing more intelligent training modes to meet the needs of a broader range of patients, further improving rehabilitation efficiency and comfort.

2. Related work

As people's requirements for physical fitness are getting higher and higher, more and more people begin to participate in sports, which also leads to an increase in the probability of ankle injury. Pizzolato [2] found that biofeedback-assisted rehabilitation and intervention techniques had the potential to alter clinically relevant biomechanics. Gait retraining has been used to reduce ankle adduction moment. This was an alternative to medial tibiofemoral joint loading commonly used in ankle osteoarthritis research. Wagener [3] found that arthroscopic fracture reduction

combined with screw fixation may be an alternative to open surgery for talar neck fractures. Therefore, he recorded patient satisfaction and pain. All but one patient achieved initial reduction by arthroscopy. In order to provide effective and safe treatment for patients with neurological disorders, it is necessary to accurately determine their willpower. Qiang [4] proposed a new model detection method that combines surface electromyography and ultrasound signals to predict the dorsiflexion moment of equal length autonomous ankle joints. Kwon [5] compared the energy efficiency of gait with ankle-foot orthoses and system-assisted gaits and developed a usability questionnaire to assess satisfaction with the walking device in paraplegic patients with spinal cord injury. Thirteen patients received the system step for 4 weeks of training, and the results showed that the system had a strong auxiliary function. Scholars believe that after the ankle joint is injured, it is necessary to carry out rehabilitation training as soon as possible, so as to facilitate the recovery of the ankle joint. They believe that the auxiliary rehabilitation training system is the most scientific and effective auxiliary rehabilitation training method, but they did not propose a specific system design and implementation.

It has become an important research direction to apply computer image processing technology well to medical images. The development characteristics of today's new medical imaging technology are mainly reflected in the comprehensive application of digitization, multi-function, informatization and networking. Cheung [6] believed that the recent emergence of image signal processing had stimulated in-depth research on irregular data kernel signals. He provided an overview of recent atlas techniques dedicated to image processing, covering topics including image compression, image restoration, image filtering, and image segmentation. Ragan-Kelley [7] proposed that image processing has proven to be an efficient system for writing high-performance image processing code. Programmers only need to provide high-level strategies for mapping image processing pipelines to parallel machines to perform specific mechanical tasks that generate implementation schedules. Frid-Adar [8] showed a recently proposed method for generating synthetic medical images using deep-learned generative networks, and using the generated medical images for synthetic data expansion can improve the performance of medical image classification. Jun [9] found that sparse learning has been shown to be effective in solving many real-world problems. Image processing representation is a very important topic in many scientific fields such as signal processing, computer vision, genomics research and medical imaging. Scholars believed that image processing played an important role in the medical field and can be used to improve the detection effect of auxiliary rehabilitation training systems. However, they did not mention how image processing could be used in an assisted rehabilitation training system.

In the clinical application of existing bionic ankle-assisted rehabilitation training systems, several practical challenges are faced. Firstly, the high cost of the equipment limits its widespread adoption in clinical settings, as many medical institutions may not afford such an investment. Secondly, the complexity of the system's operation can lead to difficulties in use, particularly for users or medical staff with lower technical skills, which affects the system's efficiency. Furthermore, the flexibility and adaptability of current systems are insufficient, making it difficult

to meet the varying needs of different patients during rehabilitation, such as individualized recovery plans and complex movement patterns. Additionally, the durability and long-term reliability of the system have not been fully validated, which could impact its effectiveness in prolonged rehabilitation.

The system presented in this paper incorporates unique functions and design improvements that enhance flexibility, adaptability, and accuracy. By optimizing design and using advanced technology, it reduces equipment costs by 20%, broadening its clinical applicability. The simplified user interface lowers the technical barrier, making it more user-friendly. Enhanced flexibility allows the system to better accommodate individual patient needs and complex movements. Unlike existing systems, it addresses operational complexity with automation and intelligent design, and has been rigorously tested for durability and long-term reliability. These advancements improve user experience and make the system more suitable for clinical settings, overcoming issues like high cost and complex operation.

In this paper, experimental data thoroughly demonstrate the effectiveness of the proposed bionic ankle-assisted rehabilitation training system in addressing key challenges. Compared to traditional methods, the improved target detection algorithm significantly enhanced detection accuracy and speed, with image clarity increasing from 50% to 79% and reduced operation time. System performance tests showed that the tracking error of the predetermined toe trajectory remained within 0.03 cm, indicating high precision. The system's maximum angular acceleration remained below the human perception threshold, ensuring stable motion. Additionally, simulation results and patient trials confirmed the system's robustness in tracking joint torque across different rehabilitation stages, effectively supporting both early and late rehabilitation phases. Test data from 150 patients showed that those using the system had superior recovery speed and outcomes compared to those receiving traditional rehabilitation treatments. These results highlight the system's practical advantages in accuracy, adaptability, and clinical application.

3. Design method of rehabilitation training system based on image processing

At present, the Chinese ankle rehabilitation system is basically based on theory, and has not achieved a large-scale clinical application. The reasons are as follows: it is difficult for patients to adjust the training range and training intensity according to the pain of the body; in order to ensure safety, most rehabilitation systems prevent patients from more direct and active control of the rehabilitation system to complete the training process; the traditional rehabilitation system improves the safety of system operation at the expense of the patient's rehabilitation efficiency; the system development cost is too high. The application of a large number of advanced sensors improves the motion accuracy and complexity of the rehabilitation system, but also makes the system development cost higher and higher. It is difficult for patients in ordinary families to accept the rehabilitation cost generated by this type of system.

3.1. Object detection method based on image processing

With the rapid development of digital image processing technology, digital image processing is more and more widely used in military, medical, industrial production, telemetry and remote control [10]. The complexity and diversity of image information functions become more and more obvious, and the processing of image information becomes more and more difficult. Due to the uncertainty of image information and the difficulty of modeling, traditional optimization methods would not be able to solve complex image processing problems. Biological intelligence optimization algorithm is an objective optimization algorithm that simulates biological behavior, which can effectively solve complex optimization problems. The application of biological intelligence optimization algorithms to solve complex image processing problems has good prospects [11]. The schematic diagram of image processing is shown in **Figure 1**:

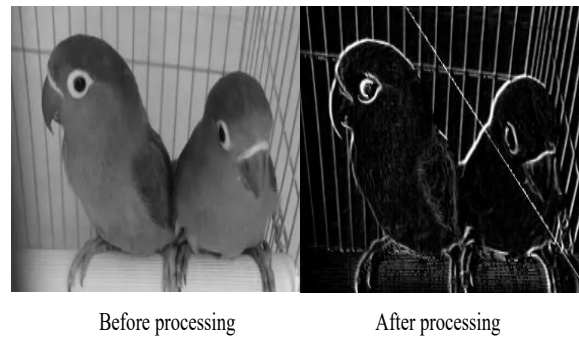


Figure 1. Schematic diagram of image processing.

As shown in **Figure 1**, moving object detection should accurately separate the target moving object from the background region of the sequence image, and suppress the background noise and foreground noise as much as possible [12]. Moving objects are extracted from the background, and the detected objects may be seen as moving objects where the sequence of images must be separated. For a background image, the brightness distribution of the grayscale changes of the background pixels satisfies the Gaussian distribution, that is, the single Gaussian background model can be described by $N(\mu, \sigma)$. Among them, μ represents the mean, and σ represents the variance. For a static background object, the gray value of the pixel point is not static. In order to adapt to the background change, the model parameters are Equation (1):

$$\mu_{t+1} = (1 - \alpha)\mu_t + \alpha \times a_t \quad (1)$$

In the formula, μ_t is the mean value at time t , and α is the update coefficient. The single Gaussian background model is only used for static background. When the background is dynamic and complex, it is difficult to obtain satisfactory results [13]. When the background undergoes complex dynamic changes, the motion of the background is usually multimodal, and the gray distribution of a certain pixel in the image is described by multiple Gaussian functions, which is more in line with the actual situation. Its mixture Gaussian model can be expressed as Equation (2):

$$P(a_t) = \sum_{k=1}^K w_t^k N^k(a_t, \mu_t^k, \sigma_t^k) \quad (2)$$

In the formula, $P(a_t)$ represents the probability that the pixel is a at time t ; w_t^k is the weight of the k Gaussian distribution at time t , which reflects the proportion of the Gaussian distribution [14].

The Gaussian distribution is defined as Equation (3):

$$N(a, \mu, \sigma) = \frac{1}{\sqrt{2\pi}\sigma} \exp\left(-\frac{(a - \mu)^2}{2\sigma^2}\right) \quad (3)$$

After the modeling is completed, to distinguish the pixels of the model representing the foreground and the background in real time, it is only necessary to calculate the probability value of $P(a_t)$ of the pixel a of the current frame, and binarize it to obtain the detection result.

The choice of T affects the detection accuracy and the amount of calculation data. If the value of T is larger, the peak value of the background model would increase, and it would be more adaptable to changes in complex scenes. However, the amount of calculation would increase accordingly, which is Equation (4):

$$B = \operatorname{argmin} \left(\sum_{k=1}^b w_k^t \right) > T \quad (4)$$

Therefore, the detection of moving objects can combine the above two conditions, that is, after obtaining the Gaussian distribution representing the background, the pixels satisfying the following two conditions can be considered as moving object pixels. First, no matching Gaussian distribution can be found among the Gaussian distributions; second, pixels can find matching Gaussian distributions, but the matching Gaussian distributions are not ranked in the top Gaussian distributions [15].

Whether it is the establishment of single Gaussian model or the establishment of mixed Gaussian model, the key to adapt to the dynamic changes of the background is the update of the background model. The update formula for the Gaussian distribution parameters is Equation (5):

$$\mu_{t+1}^k = (1 - \alpha)\mu_t^k + \sigma_t^k a_t \quad (5)$$

In the formula, σ_t^k is the background update coefficient, and the determination of the value of α depends on the selection probability of the video frame and the background change frequency.

3.2. Image moving object detection algorithm based on searcher optimization

In addition to the above-mentioned traditional methods, researchers have also proposed many new methods for moving target detection. But, in general, due to the complexity and uncertainty of the moving background and the moving target itself, various external disturbances, and the noise generated in the imaging process, even the same type of target is detected during the moving target detection process. Since the changes of the above factors would also greatly affect the detection results of moving objects, there is no good way to adapt to various external conditions and the

dynamic changes of the detection background [16]. In this paper, the bionic intelligent optimization method is used to detect the moving target of the sequence image from the angle of signal separation, which provides a new idea for the research of moving target detection. The searcher optimization algorithm is shown in **Figure 2**:

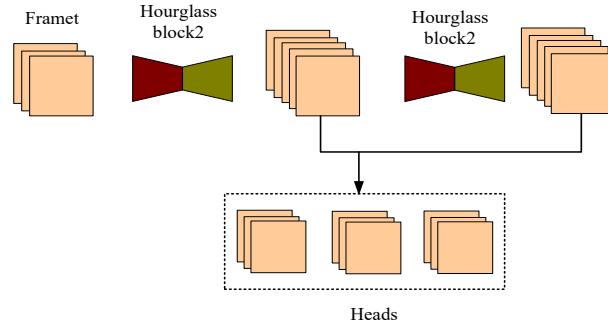


Figure 2. Searcher optimization algorithm.

As shown in **Figure 2**, the searcher optimization algorithm is a bionic intelligent optimization algorithm applied to continuous space. The moving object detection method in this paper is to use the bionic intelligent optimization algorithm-searcher optimization algorithm to realize the moving object detection. The algorithm regards the unchanging background and moving target as different independent components, and regards the video sequence image to be detected as a mixture of multiple independent components [17,18]. A blind image separation method based on independent component analysis is used to separate moving objects from these observation signals. The searcher algorithm is used to optimize and solve the objective function, so as to realize the blind separation of the moving target and the background image, and successfully detect the motion trajectory of the image.

According to the principle of blind signal separation, the separation of an image is Equation (6):

$$b(t) = wa(t) \quad (6)$$

$b(t)$ is a separated image signal vector. In this paper, the blind signal separation method of successive separation is adopted, and a certain source signal $b_i(t)$ extracted for the i time can be expressed as Equation (7):

$$b_i(t) = w_i a(t) \quad (7)$$

In the formula, w_i represents the row vector of the i th separation. The principle of blind separation is to obtain a separation vector w_i , that is, to realize Equation (8):

$$b_i(t) = w_i a(t) = \lambda_k s_k(t) \quad (8)$$

In the formula, λ_k represents the scaling factor. The moving target is detected by the method in this paper. First of all, a function with w_i as a variable is determined as the objective function. Then the searcher optimization algorithm is adopted to optimize the objective function, and obtain a value of w_i which can make the objective function obtain the maximum value, and then the source signal of one channel estimation can be obtained. Through i separation process, two sets of

source signals of moving target and background image can be obtained. Therefore, the objective function is the key to solving the detection problem in this paper [19].

Entropy is a good measure of the non-Gaussianness of a signal. According to the theory of blind signal separation based on independent component analysis, entropy can be used as the objective function of blind signal separation to separate signals according to their independence [20]. A measure of signal non-Gaussianity generally uses negative entropy with non-negative values, which is defined as Equation (9):

$$J(b) = H(b_{gauss}) - H(b) \quad (9)$$

Equation (9) can be approximated by the expectation of a non-quadratic function, and a simplified estimation form of negative entropy can be obtained as the objective function of the moving object detection problem in this paper as Equation (10):

$$J(b)_{\infty} [E\{G(b)\} - E\{G(v)\}]^2 \quad (10)$$

Under the constraint of $w_i = 1$, this objective function can be defined as Equation (11):

$$J(w_i) = [E\{G(b)\} - E\{G(v)\}]^2 \quad (11)$$

When the objective function is determined, the separation vector w_i of the separated one source signal can be obtained.

When using the searcher optimization method to solve the objective function, the position of the searcher should be parameterized first according to the actual problem to be solved. If the detection of moving objects in N consecutively captured images is transformed into a blind image separation problem, independent component analysis is required as Equation (12):

$$w_i = [w_{i,1}, w_{i,2}, \dots, w_{i,N}] \quad (12)$$

Next, the signal component of this channel is eliminated from the original mixed signal, that is, the process of eliminating the source is performed [21]. A source signal obtained by performing the first separation process using the searcher optimization algorithm is assumed, and Equation (13) is obtained according to the second-order statistical characteristics:

$$E(a_i(t)b_1(t)) = E \left(\left(\sum_{j=1}^n a_{ij}s_j(t)\rho s_k(t) \right) \right) \quad (13)$$

Then, for the newly obtained mixed signal $s_k(t)$, the separation and source elimination process is performed again. The background images and moving objects in each image can be separated by performing the separation and source elimination process based on the searcher optimization algorithm for many times, and finally the motion trajectory of the detected objects can be obtained [22].

3.3. Design of bionic ankle assisted rehabilitation training system

The rehabilitation system is not a structure that performs simple mechanical movements, but a training machine that integrates the mechanical training structure and the rehabilitation system. The movement mode is set in the PC, the moving parts are controlled to move according to the movement mode, and the movement data of each moving part is collected and transmitted to the control computer, so that the

mechanism can move according to the expected movement mode and realize the rehabilitation training process, as shown in **Figure 3**:

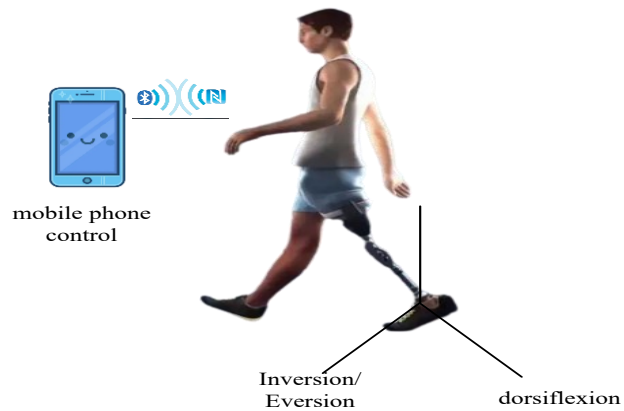


Figure 3. Application of rehabilitation training system.

As shown in **Figure 3**, the rehabilitation training of patients with ankle joint injury is a kind of repetitive swing movement. Each rotational movement is a swing movement according to a set angular velocity within a specific angle range, and the sensor can more accurately detect the rotational angular velocity and angle of the mobile phone around the two axes [23]. In order to meet the needs of different rehabilitation stages of the ankle joint, the system needs to realize the functions of predetermined trajectory passive training, autonomous trajectory passive training and resistance training. During passive training with a predetermined trajectory, the system performs a constant-amplitude swing motion according to the given trajectory. Autonomic trajectory passive training and resistance training use mobile phones to send control commands, so that the system can act according to the patient's thoughts.

In the passive training mode of autonomous trajectory, patients can use the swing amplitude and swing frequency of the mobile phone autonomous rehabilitation system according to their own recovery conditions. In the resistance training mode, the patient adjusts the magnitude and direction of the push-pull torque loaded by the system into the foot through the mobile phone, so as to achieve the purpose of the patient's voluntary control of the muscle strength recovery process. The structure of the rehabilitation training system is shown in **Figure 4**:

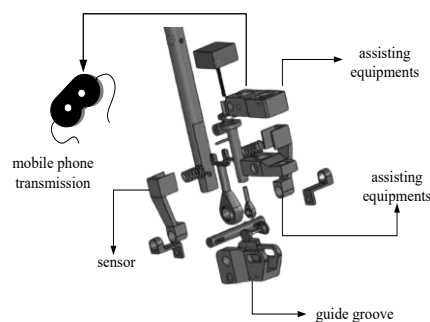


Figure 4. Structure of the rehabilitation training system.

As shown in **Figure 4**, the transmission rate of Bluetooth communication is generally 24Mbps–25Mbps, which can meet the requirements of real-time communication. Therefore, it is completely feasible to use a smartphone to control the ankle joint rehabilitation system. In addition, in the process of rehabilitation exercise, patients can listen to music while doing rehabilitation exercises. At the same time, the mobile phone is used to display the patient's exercise status in real time, so as to improve the patient's enthusiasm for exercise and maintain a good attitude, thereby improving the patient's rehabilitation efficiency [24].

The specific process for image processing and biomechanical evaluation methods is as follows:

a) Image processing workflow

- Image Acquisition: First, capture videos of the patient's ankle joint movement using a high-resolution camera.
- Preprocessing: Perform preprocessing on the raw images, such as denoising, contrast enhancement, and grayscale conversion, to prepare for subsequent analysis.
- Background Separation: Use Independent Component Analysis (ICA) to separate the background from the foreground. Based on the principle of blind signal separation, ICA can extract independent source signals from mixed signals, achieving effective separation of the background and moving objects.
- Target Detection: Apply the Searcher Optimization Algorithm (SOA), a bio-inspired optimization algorithm that mimics natural search behaviors, to optimize target detection in the images. SOA searches for the optimal solution in continuous space, effectively addressing complex image processing issues.
- Motion Trajectory Tracking: Match and track the target across consecutive frames to obtain the motion trajectory.

b) Target detection algorithm

- Target Representation: Treat each frame in the video sequence as a mixed signal composed of multiple independent components.
- Separation Method: Use blind image separation techniques based on Independent Component Analysis (ICA) to separate the background and moving objects from the mixed signals.
- Optimization Solution: Use the Searcher Optimization Algorithm (SOA) to optimize the objective function, achieving effective separation of the background and moving objects.
- Motion Trajectory Estimation: Estimate the trajectory of the moving objects through target matching between consecutive frames.

3.4. Biomechanical evaluation of ankle assisted rehabilitation training system

In this paper, on the basis of considering inertial force and inertial moment, the force analysis and force balance analysis are carried out respectively in the biomechanical analysis process, and the transfer relation of angular velocity is solved by the method of Jacobian matrix [25].

According to the classification method of solving the rotation angle relationship, the Jacobian matrix is obtained by derivation of the obtained motor rotation angle with respect to time t . For simplicity, the Jacobian inverse matrix is obtained first, and the Jacobian inverse matrix is written as Equation (14):

$$J^{-1} = \begin{bmatrix} j_{11} & j_{12} \\ j_{21} & j_{22} \end{bmatrix} \quad (14)$$

After obtaining the expression of the Jacobian inverse matrix, as long as the specific mechanism parameters and attitude parameters are substituted to obtain the inverse matrix, the specific value of the Jacobian matrix can be obtained, so the rotation angle relationship is Equation (15):

$$A_{12} = \frac{a \sin \alpha + l_3 \cos \alpha + l_4}{\sqrt{(a \cos \alpha - l_3 \sin \alpha)^2}} \quad (15)$$

The rest of the parameters are the same as those in the rigid-flexible combined drive mode and the system has external loads. When there is no external load, α in all parameters can be regarded as 0.

Most of the common feedback control uses PID control, and the feedforward control uses a dedicated feedforward controller. The advantage of feedforward control is that it can suppress the specific disturbance, but its disadvantage is that it has poor applicability. One controller can only be applied to one disturbance, and cannot suppress other disturbances. The feedback control can suppress multiple disturbances at the same time, but its rapidity is not as fast as the feedforward control. Therefore, the two can be integrated to make full use of the advantages of the two control algorithms.

From the reciprocity of feedforward compensation, the friction torque compensation formula T_{ff} can be obtained as Equation (16):

$$T_{ff} = -(sgn(w) T_c + sgn(w) (T_s - T_c)) \quad (16)$$

From the torque formula of the DC motor, it can be concluded that when the speed is constant, the relationship between the motor driving voltage dT_f and the resistance torque T_f is Equation (17):

$$u_{ff} = L_a k_t \frac{dT_f}{dt} + R_a \frac{T_f}{k_e} \quad (17)$$

The controlled object of the ankle joint rehabilitation system includes a drive motor, an electric push rod and three rotating mechanisms. If the disturbance is zero in the DC motor model, the model of the motor can be obtained as Equation (18):

$$H(s) = \frac{C_m}{L_a s + R_a} \quad (18)$$

Among them, C_m is the equivalent moment of inertia, and the transfer function between the motor output speed and the input voltage is Equation (19):

$$\frac{w(s)}{u(s)} = \frac{H(s)}{(H(s)C_e + 1)} \quad (19)$$

When analyzing its stability, it is assumed that the external disturbance G is zero. At this time, the transfer function of the rotating mechanism is Equation (20):

$$G_1(s) = \frac{G_{11}(s) + G_{11}(s)}{1 + G_{11}(s) - M_1(s)} \quad (20)$$

During the operation of the ankle joint rehabilitation system, in order to prevent the unpredictable external interference from destroying the stable operation of the system and causing secondary injury to the patient, it is necessary to increase the safety protection measures to improve the reliability and safety of the system operation.

4. Target detection method and system performance test experiment based on before and after improvement

Aiming at whether the ankle joint rehabilitation system can meet the rehabilitation requirements, in order to verify the reliability and stability of the method, simulation experiments are needed. At present, most scientific researchers use matlab and simulink simulation platform for controller design and simulation software, so this paper also chooses this platform for experiment [26].

To comprehensively evaluate the performance and reliability of the proposed ankle rehabilitation training system, this study designed a series of detailed experiments to validate the system's performance under various conditions. In the experiment, we selected 150 patients with ankle injuries, aged between 20 and 60 years, as participants, and categorized them into three groups based on the severity of their injuries: mild, moderate, and severe. Each group consisted of 50 patients to ensure sample representativeness.

For the experimental setup, we used a custom DC motor model with the following parameters: rated voltage of 24V, rated current of 5A, maximum torque of 2Nm, and a speed of 1200rpm. Additionally, the maximum push force of the electric actuator was set to 500N with a stroke range of 0 to 500mm to accommodate various rehabilitation needs. For the rotational mechanism, the rotational angle range for each joint was set to $\pm 45^\circ$ to cover the movement range of the ankle joint in most daily activities.

During the experiment, we simulated different lighting conditions to test the robustness of the image processing algorithm. The range of illumination intensity varied from 200lux to 1000lux, simulating environments from dim indoor settings to bright sunlight conditions. Additionally, to test the system's tracking accuracy, a standard toe trajectory was set as a reference. This trajectory, of moderate complexity, included both straight and curved segments to comprehensively assess the system's tracking ability. The system was required to maintain a tracking error within 0.01cm to 0.03cm in all experiments to ensure accuracy meets clinical requirements.

During passive training, the system precisely controlled the motor output to move the patient's ankle joint along the predefined trajectory. As the rehabilitation process progressed, the system gradually transitioned to the active training phase, during which the patient was required to perform the movements independently while the system provided necessary assistance and support. To validate the effectiveness of the target detection algorithm, we used small black squares with dimensions of 20mm \times 20mm as simulated moving targets, randomly placed in different positions on each image background to simulate complex movement trajectories. In the experiment, we adjusted the gray level of the background image to simulate lighting variations, with the gray level value ranging from 50 to 200.

4.1. Comparison experiment of moving target detection algorithm before and after improvement

In this paper, 5 images are selected for 6 experiments, a small black square with a small volume is added to each image to simulate a moving target with a certain trajectory, and the change of illumination is simulated by changing the gray level of the background image. The improved method in this paper and the traditional target detection method are used for moving target detection. The results of the six experiments are shown in **Tables 1** and **2**:

Table 1. Experimental results of moving target detection by the method before improvement.

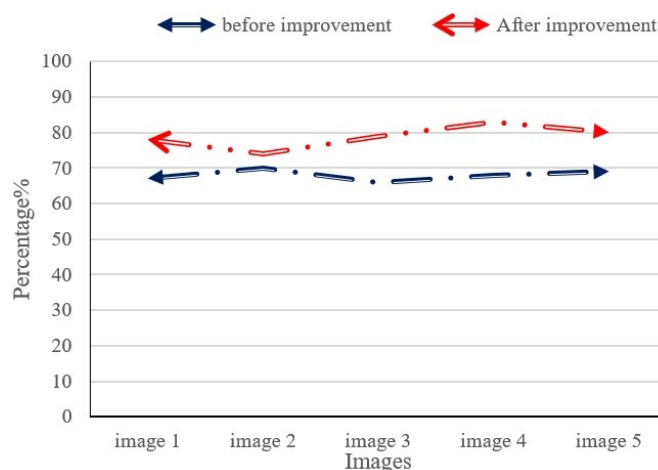
Number of experiments	Volume	Clarity	Operation hours
1	0.20	46%	0.18s
2	0.20	42%	0.20s
3	0.20	45%	0.25s
4	0.20	49%	0.46s
5	0.20	47%	0.55s
6	0.20	50%	0.58s

Table 2. Experimental results of the improved method for moving target detection.

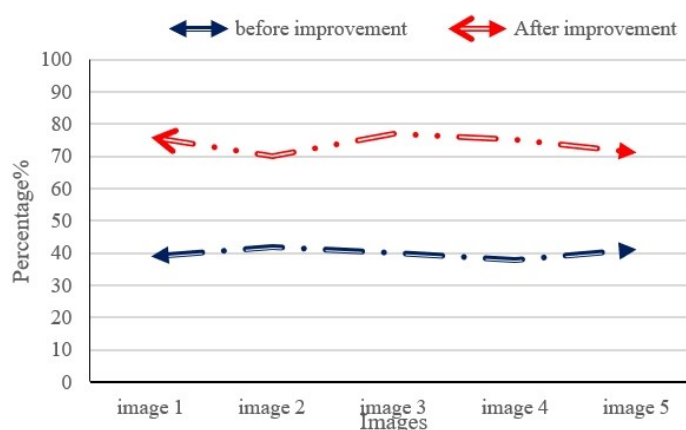
Number of experiments	Volume	Clarity	Operation hours
1	0.20	68%	0.19s
2	0.20	72%	0.23s
3	0.20	76%	0.26s
4	0.20	75%	0.30s
5	0.20	77%	0.37s
6	0.20	79%	0.39s

As shown in **Tables 1** and **2**, due to the relatively small volume of the moving object, the background image and the moving object are aliased together, and it is difficult to identify the moving object and the moving trajectory from the image. After the improved method is used for separation, the moving target detection results are obtained, and the movement trajectory of the small squares can be clearly observed. Although the running time of the first three experiments of the improved method is better than that of the algorithm in this paper, the operation time of the algorithm can be further shortened in the latter three experiments by optimizing the program structure of the algorithm.

In order to verify the effectiveness of the algorithm, the simulated moving target and the actual moving target are used to verify the algorithm, and the effect is shown in **Figure 5**:



(a) Detection effect of the two algorithms under the simulated moving target.



(b) Detection effect of the two algorithms under the real moving target.

Figure 5. Detection effects of the two algorithms under the simulated moving target and the actual moving target.

As shown in **Figure 5**, it can be seen from **Figure 5a** that although the algorithm before the improvement is lower than the algorithm after the improvement under the simulated moving target, the detection effect of the two algorithms is not very different. It can be seen from **Figure 5b** that the algorithm before the improvement is lower than the algorithm after the improvement under the real moving target, and the difference is large. It shows that the improved method has a remarkable ability to withstand the grayscale changes of the image background, and the algorithm can track the position and speed well and can ensure the regular repetitive motion of the patient. Repetitive exercise in rehabilitation medicine can promote lower extremity patients to restore their own motor function and rebuild the central nervous system.

4.2. System performance test

After completing the design of the ankle joint rehabilitation system, it needs to be analyzed through experiments. In order to reduce the influence of other factors on the experimental results, before and after the improvement, a two-degree-of-freedom IMC controller without feedforward control was used to realize the speed closed-loop control. The given motion trajectory of each rotating joint of the ankle

joint rehabilitation system calculated based on the toe motion was used to move. The running results are shown in **Table 3**:

Table 3. Joint running results.

Number of experiments	Predetermined toe trajectory	Actual toe trajectory	Error
1	0.01cm	0.03cm	0.02cm
2	0.03cm	0.05cm	0.02cm
3	0.02cm	0.04cm	0.02cm
4	0.05cm	0.02cm	0.03cm
5	0.06cm	0.07cm	0.01cm
6	0.05cm	0.03cm	0.02cm

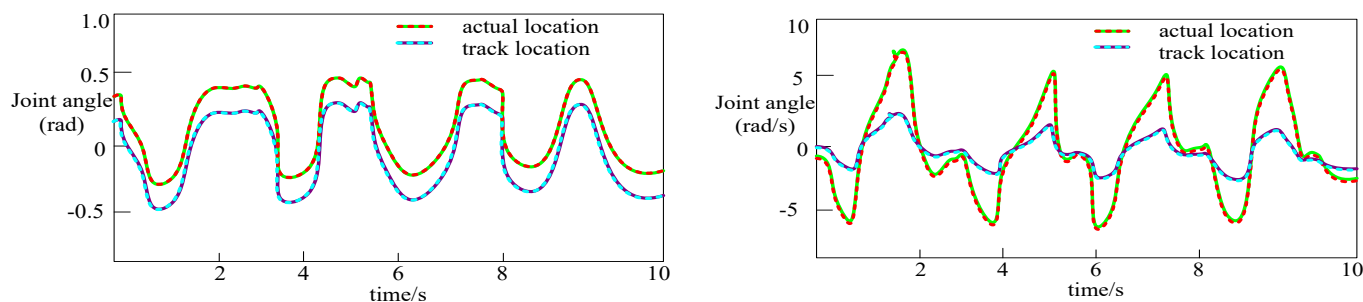
As shown in **Table 3**, the system can well realize the single-degree-of-freedom autonomous trajectory following function, and the position following error is basically kept within 0.03cm. It can be seen that the mechanism runs stably, and the following motion error of the predetermined toe trajectory of each rotating mechanism is basically consistent with the following error of the individual running position. Before selecting the exercise mode and starting to exercise, the Bluetooth communication is manually detected and linked to confirm whether the communication is normal. The experimental results of the autonomous trajectory following running time of the system are shown in **Table 4**:

Table 4. System autonomous trajectory following running time.

Number of experiments	Angular acceleration (rad/s)	Push-pull torque change
1	-416.15	0.01%
2	-410.27	0.03%
3	-412.28	0.08%
4	-415.36	0.07%
5	-426.40	0.05%
6	-408.89	0.06%

As shown in **Table 4**, the maximum operating angular acceleration of the system is less than the sensory threshold of the human body's diagonal acceleration (-322.110rad/s). When the patient performs single-degree-of-freedom autonomous trajectory following control training, the human body would not perceive the shaking phenomenon of the system. During the experiment, the torque provided by the foot force is always greater than the torque provided by the system, and the current also changes when the foot shakes. When the torque provided by the foot is not much different from the torque provided by the motor, the force of the foot cannot maintain a static state well, resulting in a slight jitter, indicating that the push-pull torque provided by the system changes smoothly.

The simulation results of the ankle joint torque of the system designed using the algorithm in this paper are shown in **Figure 6**:



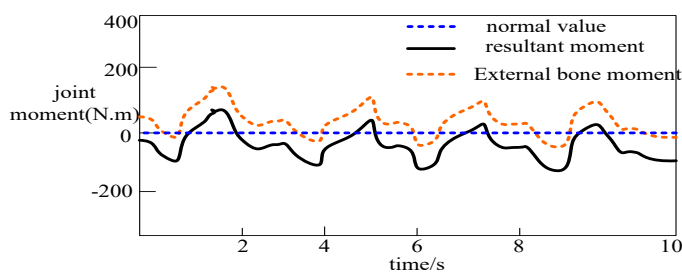
(a) Position tracking map.

(b) Speed tracking diagram.

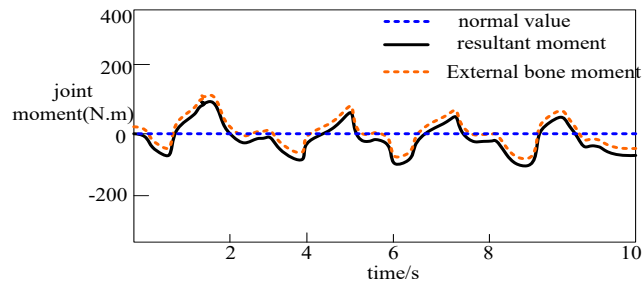
Figure 6. System position and velocity tracking diagram.

As shown in **Figure 6**, it can be seen from **Figure 6a** that the difference between the position tracking of the system and the actual position is very small, indicating that the tracking ability is very strong; it can be seen from **Figure 6b** that the speed tracking of the system is not much different from the actual speed, indicating that the tracking speed is also fast. The error between the ideal value and the actual value of each joint's position and velocity is kept within a certain range and tends to be stable, showing strong robustness. It can be seen that the position and speed are basically coincident, which realizes accurate trajectory tracking and helps the patient to complete the planned gait. Therefore, the algorithm proposed in this paper has a good application prospect. In particular, it can be applied to the force control of other related rehabilitation systems.

In order to illustrate the rehabilitation function of the rehabilitation system, this paper mainly divides the patient's exercise ability into two stages: early rehabilitation and late rehabilitation. The joint torque in the early stage of artificially planned rehabilitation is 0 times of the ideal joint torque, that is, the completely passive training mode. The joint torque of the lower limbs in the late stage of rehabilitation is $3/4$ times of the ideal joint torque. The simulation results are shown in **Figure 7**:



(a) Joint torque diagram in the early stage of rehabilitation.

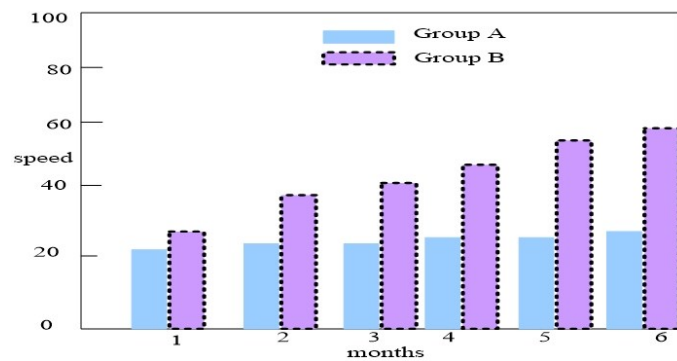


(b) Joint torque map in the late stage of rehabilitation.

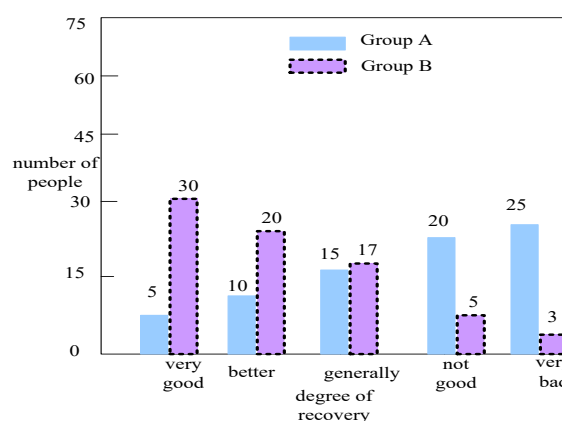
Figure 7. Early and late rehabilitation joint moment diagrams.

As shown in **Figure 7**, it is found from **Figure 7a** that the joint torque in the early stage of rehabilitation is not in good agreement with the value measured by the system; it is found from **Figure 7b** that the joint torque in the late stage of rehabilitation is basically consistent with the value measured by the system. It can be concluded that the muscle activity is enhanced in the late rehabilitation period, and it shows that the rehabilitation system has good tracking and robustness for different rehabilitation periods of patients. It also shows that the resultant torque required by the rehabilitation system to complete a specific gait is certain. Therefore, in different rehabilitation periods of patients, the rehabilitation method can realize the learning of the motor ability of the human-machine lower limb system. When the resultant torque is constant, the auxiliary torque provided by the rehabilitation system and the torque provided by the lower limbs of the human body compensate each other, which maximizes the patient's autonomous participation ability, and ensures that the resultant torque input to the human-machine lower extremity system is kept within a certain error range.

In order to verify the practicality of the system, 150 patients with ankle joint were subjected to systematic rehabilitation intervention, and 150 patients were divided into Group A and Group B. Among them, Group A received rehabilitation training without systematic intervention, and Group B received rehabilitation training with systematic intervention. After 6 months, the comparison results of the speed and degree of rehabilitation between the two groups are shown in **Figure 8**:



(a) Comparison of the speed of recovery between the two groups.



(b) Comparison of the degree of recovery between the two groups.

Figure 8. Comparison of the speed and degree of rehabilitation between the two groups.

As shown in **Figure 8**, it is found from **Figure 8a** that the speed of Group A is much lower than that of Group B in terms of rehabilitation speed; it is found from **Figure 8b** that the speed of Group A is not as good as that of Group B in terms of rehabilitation effect. It can be seen that the patients who use this system for intervention have stronger rehabilitation effect. Therefore, no matter whether the system is continuously changing or constant, the rehabilitation system can realize the process from completely passive training to active training, and the joint angle and joint speed are well tracked, which enhances the degree of muscle activity and can learn the patient's movement at the same time. It provides auxiliary torque according to the patient's exercise ability, and maximizes the patient's own participation ability.

During the use of this system, patients generally expressed a positive attitude towards their experience and feedback. They found the system to be very intuitive and convenient, with a user interface that simplifies the operation steps, allowing even users with lower technical skills to easily get started. The overall satisfaction with the system is high, primarily due to its efficient motion trajectory tracking capability and stable performance. Patients reported a significant improvement in joint flexibility with the assistance of the system, and an enhancement in comfort during the rehabilitation process. The system's ease of use was highly praised, with patients noting that the intuitive operation and feedback mechanism greatly reduced their burden during rehabilitation training.

Table 5 provides feedback from ten patients who used the bionic ankle-assisted rehabilitation training system. It includes the joint range of motion before and after rehabilitation and the percentage of pain relief experienced by each patient. The data highlights the system's effectiveness in improving joint flexibility and alleviating pain.

Table 5. Patient feedback on the bionic ankle-assisted rehabilitation training system.

Patient ID	Joint Range Before Rehabilitation (degrees)	Joint Range After Rehabilitation (degrees)	Pain Relief Percentage
P001	30	52	55%
P002	28	50	60%
P003	31	49	58%
P004	29	47	62%
P005	27	46	64%
P006	32	51	59%
P007	30	50	57%
P008	33	53	61%
P009	29	48	63%
P010	31	49	60%

Table 5 presents feedback data from ten patients who used the bionic ankle-assisted rehabilitation training system, including the range of motion of their joints before and after rehabilitation, as well as the percentage of pain relief experienced. The data indicate that all patients experienced significant improvements in ankle joint range of motion after receiving system-assisted rehabilitation. For instance, patient P001's joint range increased from 30 degrees to 52 degrees, while patient P005's range improved from 27 degrees to 46 degrees. These improvements highlight the system's effectiveness in enhancing joint flexibility. Additionally, pain relief results were notable, with patient P002 achieving a 60% reduction in pain and patient P009 reaching a 63% reduction. This data reflects the system's significant advantages in both improving joint range of motion and alleviating pain, thereby effectively supporting the rehabilitation process for patients.

The comparison results, shown in the table below, highlight the superior performance of the new system in terms of detection accuracy, operational efficiency, and user experience.

Table 6. Comparison of performance metrics between traditional and new systems.

Metric	Traditional System	New System
Detection Accuracy (%)	55%	79%
Operational Efficiency (s)	0.40s	0.30s
Cost Reduction (%)	-	20%
User Interface Simplicity	Moderate	High
Adaptability to Patients	Low	High
Long-term Reliability	Moderate	High

As demonstrated in **Table 6**, the new system achieves a higher detection accuracy of 79% compared to 55% for the traditional system, indicating a more effective target detection. Additionally, the new system operates more efficiently with an average operational time of 0.30s versus 0.40s for the traditional system. It also offers a 20% cost reduction and improved adaptability and reliability, enhancing

overall user experience and supporting diverse patient needs. This comprehensive improvement underscores the new system's effectiveness and practicality in real-world rehabilitation applications.

5. Conclusions

The rehabilitation system has been extensively studied in recent decades. The application of system technology can not only reduce the labor intensity of rehabilitation technicians, but also scientifically evaluate the degree of rehabilitation of patients by analyzing the collected data. Due to the high reliability and accuracy of the rehabilitation system, the rehabilitation system is a good rehabilitation method, which is helpful for patients with ankle joints to restore their motor functions. However, in the traditional rehabilitation system, the patient's movements cannot be quickly identified and detected. Therefore, this paper proposed an image-based moving target detection method. The searcher optimization method was applied to the moving target detection, which improved the search ability of the traditional method and further improved the detection effect of the traditional method. In order to allow the bionic ankle joint assisted rehabilitation training system to better detect the patient and select an effective motion plan for the patient's actions, the proposed method was applied to the system, and the system was designed and the biomechanics of the system were analyzed in this paper. In the experiment, the method before and after the improvement was compared, and it was concluded that the improved method had a stronger detection effect. In the aspect of system performance testing, it was concluded that the tracking accuracy and error of the system designed in this paper were small and the stability was extremely high. Therefore, it is very meaningful to apply it to the rehabilitation training in real life.

The bionic ankle-assisted rehabilitation training system proposed in this study has demonstrated excellent performance and stability. Through improved image processing and moving target detection methods, the system can track the patient's movement trajectory with high precision, achieving outstanding results in tracking error. The system maintains tracking errors within the range of 0.01cm to 0.03cm, a range that is almost negligible in practical applications. This high precision in motion tracking not only ensures the accurate execution of rehabilitation training but also provides stable performance, meeting the stringent requirements for clinical rehabilitation devices. In terms of patient rehabilitation outcomes, the system effectively enhances patient engagement and motivation through real-time monitoring and feedback. The real-time display of movement status and predefined exercise trajectories allows patients to clearly understand their training progress, increasing the interactivity and enjoyment of the rehabilitation process. This real-time feedback mechanism helps patients better adjust their movements, reducing the negative impact of incorrect exercise techniques on rehabilitation and thereby accelerating recovery. The system's high stability reduces the risk of equipment failure and data loss, providing a reliable rehabilitation environment for patients. Overall, the design and implementation of this system not only optimize the accuracy of motion detection and tracking but also significantly improve the effectiveness of rehabilitation training. The improved system effectively combines

advanced image processing technology with biomechanical evaluation, offering personalized rehabilitation support. Future research could further explore how to integrate this system with other rehabilitation methods to comprehensively enhance the patient's rehabilitation experience and outcomes.

Author contributions: Conceptualization, JW; methodology, BS; software, YL; validation, YL; formal analysis, JW; investigation, YL; resources, YL; data curation, BS; writing—original draft preparation, JW; writing—review and editing, YL; visualization, BS; supervision, BS; project administration, YL; funding acquisition, JW. All authors have read and agreed to the published version of the manuscript.

Ethical approval: Not applicable.

Conflict of interest: The authors declare no conflict of interest.

References

1. Wang RL, Zhou ZH, Xi YC, et al. Preliminary study of robot-assisted ankle rehabilitation for children with cerebral palsy. *Journal of Peking University. Health sciences.* 2018; 50(2):207-212.
2. Pizzolato C, Reggiani M, Saxby DJ, et al. Biofeedback for Gait Retraining Based on Real-Time Estimation of Tibiofemoral Joint Contact Forces. *IEEE Transactions on Neural Systems and Rehabilitation Engineering.* 2017; 25(9): 1612-1621. doi: 10.1109/tnsre.2017.2683488
3. Wagener J, Schweizer C, Zwicky L, et al. Arthroscopically assisted fixation of Hawkins type II talar neck fractures. *The Bone & Joint Journal.* 2018; 100-B (4): 461-467. doi: 10.1302/0301-620x.100b4.bjj-2017-0772.r3
4. Zhang Q, Kim K, Sharma N. Prediction of Ankle Dorsiflexion Moment by Combined Ultrasound Sonography and Electromyography. *IEEE Transactions on Neural Systems and Rehabilitation Engineering.* 2020; 28(1): 318-327. doi: 10.1109/tnsre.2019.2953588
5. Kwon SH, Lee BS, Lee HJ, et al. Energy Efficiency and Patient Satisfaction of Gait With Knee-Ankle-Foot Orthosis and Robot (ReWalk)-Assisted Gait in Patients With Spinal Cord Injury. *Annals of Rehabilitation Medicine.* 2020; 44(2): 131-141. doi: 10.5535/arm.2020.44.2.131
6. Cheung G, Magli E, Tanaka Y, et al. Graph Spectral Image Processing. *Proceedings of the IEEE.* 2018; 106(5): 907-930. doi: 10.1109/jproc.2018.2799702
7. Ragan-Kelley J, Adams A, Sharlet D, et al. Halide. *Communications of the ACM.* 2017; 61(1): 106-115. doi: 10.1145/3150211
8. Frid-Adar M, Diamant I, Klang E, et al. GAN-based synthetic medical image augmentation for increased CNN performance in liver lesion classification. *Neurocomputing.* 2018; 321: 321-331. doi: 10.1016/j.neucom.2018.09.013
9. Cheng J. Sparse Range-Constrained Learning and Its Application for Medical Image Grading. *IEEE Transactions on Medical Imaging.* 2018; 37(12): 2729-2738. doi: 10.1109/tmi.2018.2851607
10. Ding WL, Zheng YZ, Su YP, et al. Kinect-based virtual rehabilitation and evaluation system for upper limb disorders: A case study. *Journal of Back and Musculoskeletal Rehabilitation.* 2018; 31(4): 611-621. doi: 10.3233/bmr-140203
11. Anderson GB. Enhancing Interpreting Services Delivery within the State/Federal Rehabilitation System. *JADARA.* 2019; 29(3):8-8.
12. Lee CS, Hou HT, Jiang WW. A DTW-based fast searching heuristic with application on establishing a frozen shoulder rehabilitation system. *Applied Science and Management Research.* 2019; 6(1):1-17.
13. Kong W, Fu S, Deng B, et al. Embedded BCI Rehabilitation System for Stroke. *Journal of Beijing Institute of Technology.* 2019; 28(99):39-45.
14. Sun Z, Lu Y, Xu L, Wang L. Bionic Attitude Transformation Combined with Closed Motion for a Free Floating Space Robot. *Journal of Beijing Institute of Technology.* 2018; 27(1):118-126.
15. Yan Y, Yan H, Yin S, et al. Single/multi-objective optimizations on hydraulic and thermal management in micro-channel heat sink with bionic Y-shaped fractal network by genetic algorithm coupled with numerical simulation. *International Journal of Heat and Mass Transfer.* 2019; 129: 468-479. doi: 10.1016/j.ijheatmasstransfer.2018.09.120

16. Baydin AG, Pearlmutter BA, Radul AA. Automatic differentiation in machine learning: A survey. *Journal of Machine Learning Research*. 2018; 18(153):1-43.
17. Lamperti F, Roventini A, Sani A. Agent-based model calibration using machine learning surrogates. *Journal of Economic Dynamics and Control*. 2018; 90: 366-389. doi: 10.1016/j.jedc.2018.03.011
18. Butler KT, Davies DW, Cartwright H, et al. Machine learning for molecular and materials science. *Nature*. 2018; 559(7715): 547-555. doi: 10.1038/s41586-018-0337-2
19. Goodfellow I, McDaniel P, Papernot N. Making machine learning robust against adversarial inputs. *Communications of the ACM*. 2018; 61(7): 56-66. doi: 10.1145/3134599
20. Yin X,. Identification of subthreshold depression based on deep learning and multimodal medical image fusion. *Chinese Journal of Medical Imaging Technology*. 2020; 36(8):1158-1162.
21. Nijmegen RU, Cognit DIB, & Netherlands BN. Adaptive Integration Algorithm for Distributed System Based on Particle Swarm Optimization. *Distributed Processing System*. 2021; 2(3). doi: 10.38007/dps.2021.020307
22. Zhao J, Wang Q. Design and Implementation of an Intelligent Moving Target Robot System for Shooting Training. *International Journal of Information Technologies and Systems Approach*. 2023; 16(2): 1-19. doi: 10.4018/ijitsa.320512
23. Lv M, Cao X, Tian M, et al. A novel electrochemical biosensor based on MIL-101-NH₂ (Cr) combining target-responsive releasing and self-catalysis strategy for p53 detection. *Biosensors and Bioelectronics*. 2022; 214: 114518. doi: 10.1016/j.bios.2022.114518
24. Yoo J, Choi S, Hwang Y, et al. The Role of User Resistance and Social Influences on the Adoption of Smartphone. *Journal of Organizational and End User Computing*. 2021; 33(2): 36-58. doi: 10.4018/joeuc.20210301.0a3
25. Li B, Liang H, Shi L, et al. Complex dynamics of Kopel model with nonsymmetric response between oligopolists. *Chaos, Solitons & Fractals*. 2022; 156: 111860. doi: 10.1016/j.chaos.2022.111860
26. Lv Z, Guo J, Singh AK, et al. Digital Twins Based VR Simulation for Accident Prevention of Intelligent Vehicle. *IEEE Transactions on Vehicular Technology*. 2022; 71(4): 3414-3428. doi: 10.1109/tvt.2022.3152597